

## Serum cholesterol and variant in cholesterol-related gene *CETP* predict white matter microstructure



Nicholus M. Warstadt<sup>a</sup>, Emily L. Dennis<sup>a</sup>, Neda Jahanshad<sup>a</sup>, Omid Kohannim<sup>b</sup>, Talia M. Nir<sup>a</sup>, Katie L. McMahon<sup>c</sup>, Greig I. de Zubicaray<sup>d</sup>, Grant W. Montgomery<sup>e</sup>, Anjali K. Henders<sup>e</sup>, Nicholas G. Martin<sup>e</sup>, John B. Whitfield<sup>e</sup>, Clifford R. Jack Jr.<sup>f</sup>, Matt A. Bernstein<sup>f</sup>, Michael W. Weiner<sup>g,h</sup>, Arthur W. Toga<sup>i</sup>, Margaret J. Wright<sup>d,e</sup>, Paul M. Thompson<sup>a,b,\*1</sup>, for the Alzheimer's Disease Neuroimaging Initiative (ADNI)<sup>1</sup>

<sup>a</sup> Imaging Genetics Center, Institute for Neuroimaging and Informatics, Keck School of Medicine of the University of Southern California, Los Angeles, CA, USA

<sup>b</sup> Department of Neurology, UCLA School of Medicine, Los Angeles, CA, USA

<sup>c</sup> Centre for Advanced Imaging, University of Queensland, Brisbane, Australia

<sup>d</sup> School of Psychology, University of Queensland, Brisbane, Australia

<sup>e</sup> Queensland Institute of Medical Research Berghofer Medical Research Institute, Brisbane, Australia

<sup>f</sup> Department of Radiology, Mayo Clinic and Foundation, Rochester, MN, USA

<sup>g</sup> Department of Radiology and Biomedical Imaging, UCSF School of Medicine, San Francisco, CA, USA

<sup>h</sup> Veteran Affairs Medical Center, San Francisco, CA, USA

<sup>i</sup> Laboratory of Neuro Imaging, Institute for Neuroimaging and Informatics, USC Keck School of Medicine, Los Angeles, CA, USA

### ARTICLE INFO

#### Article history:

Received 21 October 2013

Received in revised form 21 May 2014

Accepted 26 May 2014

Available online 2 June 2014

#### Keywords:

Brain structure

DTI

Imaging genetics

Cholesterol

Development

Aging

### ABSTRACT

Several common genetic variants influence cholesterol levels, which play a key role in overall health. Myelin synthesis and maintenance are highly sensitive to cholesterol concentrations, and abnormal cholesterol levels increase the risk for various brain diseases, including Alzheimer's disease. We report significant associations between higher serum cholesterol (CHOL) and high-density lipoprotein levels and higher fractional anisotropy in 403 young adults ( $23.8 \pm 2.4$  years) scanned with diffusion imaging and anatomic magnetic resonance imaging at 4 Tesla. By fitting a multi-locus genetic model within white matter areas associated with CHOL, we found that a set of 18 cholesterol-related, single-nucleotide polymorphisms implicated in Alzheimer's disease risk predicted fractional anisotropy. We focused on the single-nucleotide polymorphism with the largest individual effects, *CETP* (rs5882), and found that increased G-allele dosage was associated with higher fractional anisotropy and lower radial and mean diffusivities in voxel-wise analyses of the whole brain. A follow-up analysis detected white matter associations with rs5882 in the opposite direction in 78 older individuals ( $74.3 \pm 7.3$  years). Cholesterol levels may influence white matter integrity, and cholesterol-related genes may exert age-dependent effects on the brain.

© 2014 Elsevier Inc. All rights reserved.

### 1. Introduction

Nearly a quarter of the body's cholesterol lies in the central nervous system (CNS) (Dietschy and Turley, 2004), where it serves as the rate-limiting factor for myelin biosynthesis (Saher et al., 2005). The available pool of cholesterol in the brain also governs CNS synaptogenesis (Mauch et al., 2001). Thus, cholesterol is essential for brain maturation and white matter (WM) development, and decreased cholesterol early in life may limit both the number and efficacy of synapses. CNS cholesterol concentration is largely independent of serum cholesterol levels because of the low permeability of cholesterol through the blood brain barrier

\* Corresponding author at: Imaging Genetics Center, Institute for Neuroimaging and Informatics, Keck School of Medicine, University of Southern California, 2001 N. Soto Street, Los Angeles, CA 90033, USA. Tel.: +1 323 442 7246; fax: +1 323 442 7247.

E-mail address: [pthomp@usc.edu](mailto:pthomp@usc.edu) (P.M. Thompson).

<sup>1</sup> Many other investigators within the Alzheimer's Disease Neuroimaging Initiative (ADNI) contributed to the design and implementation of ADNI and/or provided data, but most of them did not participate in analysis or writing of this report. A complete list of ADNI investigators may be found at: [http://adni.loni.usc.edu/wp-content/uploads/how\\_to\\_apply/ADNI\\_Acknowledgement\\_List.pdf](http://adni.loni.usc.edu/wp-content/uploads/how_to_apply/ADNI_Acknowledgement_List.pdf).

(Saher and Simons, 2010). Even so, changes in serum concentrations have been associated with variations in the healthy brain's WM structure (Cohen et al., 2011; Williams et al., 2013).

The WM fiber structure of the living human brain can be assessed noninvasively using diffusion tensor imaging (DTI). DTI has been used to both characterize patterns of the developing brain (Hüppi and Dubois, 2006; Tamnes et al., 2010) and to demonstrate differences between healthy and unhealthy brains in many disease processes (Le Bihan et al., 2001; Nir et al., 2013). Regional differences in DTI-derived WM metrics are highly heritable (Jahanshad et al., 2013; Jin et al., 2011; Thomason and Thompson, 2011) and are associated with differences in a variety of factors including serum biomarker measures (Jahanshad et al., 2012) and cognitive performance (Chiang et al., 2009; Grieve et al., 2007; Kochunov et al., 2010).

Variations in plasma lipid and lipoprotein levels are also highly heritable, and differences even within the healthy range of cholesterol values may exert influence over the brain. A range of 40%–60% of the normal variation in total cholesterol (CHOL), high-density lipoprotein (HDL), and low-density lipoprotein (LDL) concentrations are attributable to genetic influences (Asselbergs et al., 2012), and several genetic variants have been identified that are associated with lipoprotein levels (Asselbergs et al., 2013). Cholesterol levels may have age-dependent effects on cognition, suggesting a changing need for cholesterol in the brain over the life span. Multiple studies suggest that higher cholesterol levels in younger adults may be associated with higher fluid intelligence (speed and/or flexibility of mental processing) (Waldstein and Elias, 2001). Specifically, university undergraduate students with higher serum cholesterol levels showed faster decision-making and movement times on a choice reaction time test (Benton, 1995), and non-elderly adults with higher cholesterol levels performed better on the WAIS-R Block Design test, which requires rapid, adaptive problem solving skills (Waldstein and Elias, 2001). Although some studies similarly correlate lower cholesterol with poorer executive function in older adults (Elias et al., 2005; Manolio et al., 1993), late-life hypercholesterolemia has been strongly associated with an increased risk for Alzheimer's disease (AD) (Refolo et al., 2000; Shobab et al., 2005), a neurodegenerative disease characterized by cognitive deficit (Derouesné et al., 1999). In general, faster processing and motor speeds have been associated with higher fractional anisotropy (FA) (Aukema et al., 2009; Chiang et al., 2009), and poorer cognitive performance in executive tasks has been associated with lower FA (Grieve et al., 2007). As cognition has been associated with cholesterol levels as well as differences in WM, we hypothesize that cholesterol concentration also predicts white matter microstructure.

Currently, the role of the serum cholesterol and cholesterol gene variants on brain development and risk for disease are not well understood. As WM continues to mature beyond age 30 (Bartzokis et al., 2004; Kochunov et al., 2010; Tamnes et al., 2010), we set out to determine whether serum cholesterol concentrations measured during adolescence (mean age: 15 years) might predict WM integrity almost a decade later in early adulthood (mean age: 24 years) in a large cohort of 403 healthy individuals. We further hypothesized that genetic risk factors for high cholesterol, particularly those with known neurologic associations, might relate to WM microstructure - estimated using FA and mean, radial, and axial diffusivities - and that these same specific genetic variants would be associated with axonal integrity in an independent sample of elderly adults. Our goal was to determine if serum cholesterol levels and common cholesterol-related genetic variants were associated with WM microstructural integrity, and, further, if the relationship differed in younger and older age groups.

## 2. Methods

We examined 2 different cohorts—the Queensland Twin IMaging cohort (QTIM) of young Australian twins and elderly individuals scanned across North America as part of the Alzheimer's Disease Neuroimaging Initiative (ADNI). An overview of the analyses performed in each of these cohorts is summarized in [Supplementary Fig. 1](#).

### 2.1. QTIM cohort

The QTIM study is a project recruiting healthy Australian twins to identify genes influencing brain health and to better understand genetic factors that affect the brain. Participants were excluded if they had a history of significant head injury, neurologic or psychiatric illness, substance abuse or dependence, or had a first-degree relative with a psychiatric disorder. Participant performance was also assessed over a range of cognitive tasks. Handedness was assessed using 12 items from Annett Handedness Questionnaire (Annett, 1970). Our study included 403 right-handed, Caucasian participants (146 men and 257 women). Their mean age was 23.8 years (standard deviation, SD: 2.4).

### 2.2. Determining cholesterol levels

Multiple (average 2.2, SD 1.0) non-fasting serum cholesterol samples were collected from participants scanned in the QTIM study. Lipid measurements were assessed at 12, 14, and/or 16 years. If multiple measures were available for any given subject, the cholesterol values and ages at measurement were averaged. The participants' mean age at the time of the cholesterol measurements was 15.2 years (SD 2.3). The lipid panel directly measured CHOL, HDL, and triglyceride levels; LDL was indirectly calculated (and will thus be referred to as LDL-c) from the Friedewald equation (Warnick et al., 1990):

$$LDL - c = CHOL - HDL - (Triglycerides/5) \quad (1)$$

Measuring lipid levels in the fasting state is typical, but some studies argue that this may be detrimental to accurate risk assessment based on the lipid profile (Langsted et al., 2008; Mora et al., 2008). Proponents of fasting lipid measurements often cite the increase in triglyceride levels during a fat tolerance test as a source of error (Schaefer et al., 2001). In a study of 33,391 individuals, Langsted et al. (2008) reported that non-fasting levels of lipids, lipoproteins, and apolipoproteins vary only minimally from levels in the fasting state. Furthermore, multiple averaged non-fasting measures may better reflect the body's typical lipid profile, as more time is spent in the post-absorptive state than the "fasting" state. In the same study, non-fasting LDL-c differed only slightly from fasting measures, but was more useful for predicting risk of cardiovascular events. Thus, non-fasting CHOL, HDL, and LDL-c were all analyzed in the present study.

### 2.3. Selection of genes of interest

In a genome-wide association study of 66,240 individuals, Asselbergs et al. (2012) found 945 single-nucleotide polymorphisms (SNPs) involved in cholesterol metabolism, 170 of which were genotyped as part of the Illumina Quad-610 BeadChip in our QTIM cohort (genotyping protocol is available in the [Supplementary Methods](#)). We eliminated SNPs with a minor allele frequency <0.22 or a linkage disequilibrium >0.4 to assure that the homozygous minor allele carriers always represented at least 5% of our population and that associations found were independent of variations in other SNPs included in the model. All SNPs passing the

**Table 1**

Summary of SNPs included in our multi-SNP analysis

SNP	Nearest gene	MAF	Minor allele
rs102275	<i>FADS1</i>	0.483	C
rs11206514	<i>PCSK9</i>	0.4093	C
rs2000069	<i>ABCA1</i>	0.4863	T
rs253	<i>LPL</i>	0.4959	T
rs261341	<i>LIPC</i>	0.4597	A
rs3846662	<i>HMGCR</i>	0.4158	G
rs387976	<i>PVRL2</i>	0.4734	C
rs405509	<i>TOMM40</i>	0.4927	T
rs439401	<i>APOE</i>	0.3942	T
rs4810479	<i>PLTP</i>	0.4226	C
rs4970843	<i>SORT1</i>	0.4245	C
rs55882	<i>CETP</i>	0.4478	G
rs5930	<i>LDLR</i>	0.3494	A
rs6602910	<i>GAS6</i>	0.4588	T
rs7120118	<i>NR1H3</i>	0.4634	C
rs7122944	<i>PAFAH1B2</i>	0.2289	G
rs783149	<i>LPA</i>	0.3155	A
rs838878	<i>SCARB1</i>	0.3397	A

SNPs included in the multi-SNP model. The gene (or the nearest gene when SNP is intergenic), minor allele frequency and minor allele associated with cholesterol for each SNP.

Key: MAF, minor allele frequency; SNP, single-nucleotide polymorphism.

initial inclusion criteria (genotyped with passing minor allele frequencies and linkage disequilibriums) were included in keyword searches using Google Scholar to search for prior reports of associations with AD. Of these, 18 SNPs had been associated with AD and were included as SNPs of interest in our study (Astarita et al., 2010; Baum et al., 1999; Dzamko et al., 2011; Gustafsen et al., 2013; Ikeda and Yamada, 2010; Kysenius et al., 2012; Lamsa et al., 2008; Mulder et al., 2012; Natunen et al., 2012; Page et al., 2012; Rodriguez-Rodriguez et al., 2009; Roses et al., 2010; Solfrizzi et al., 2002; Vuletic et al., 2003; Wollmer et al., 2003; Xiao et al., 2012). The SNPs we included are summarized in Table 1.

These 18 cholesterol-Alzheimer's disease risk SNPs were then entered into a multi-locus analysis to examine whether they had a collective effect in predicting white matter microstructural integrity. A general flow diagram of our hypotheses is shown in Fig. 1.

#### 2.4. Cholesterol analysis

A random-effects model (to account for family relatedness) was used to study the statistical significance of plasma cholesterol values (CHOL, HDL, and LDL-c) voxelwise on regional white matter, while covarying for age and sex. Multiple comparisons corrections were used to control for false positives.

#### 2.5. Multi-SNP analysis

Linear mixed-effects models were used to study the joint associations of SNPs with imaging measures (Kohannim et al., 2012), accounting for kinship among participants using the efficient mixed-model association (EMMA; <http://mouse.cs.ucla.edu/emma/>) software with restricted maximum likelihood estimation (Kang et al., 2008). This analysis was carried out within the voxels associated with CHOL in the previous analysis. Arguably, the effects of cholesterol-related SNPs on the brain may be more likely to be detected at locations where serum cholesterol associations have already been detected. Such a relationship was found in a voxel-wise FA analysis of serum iron transport protein levels and related genes (Jahanshad et al., 2012). A restricted search space imposes a less stringent significance threshold to report credible associations. Otherwise a heavy multiple comparisons correction is required to adjust for searching the whole brain.

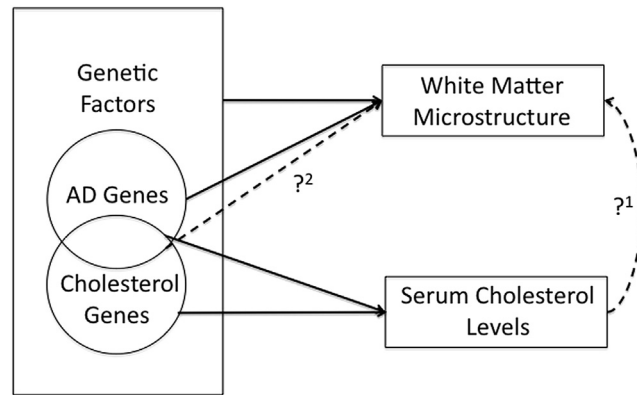


**Fig. 1.** Overview of the motivating factors for our study, including the current understanding of cholesterol's relationship to the brain and hypotheses that our study aimed to test. Several known relationships (solid black arrows) motivated our study. Both serum cholesterol levels and brain structure are highly heritable. In our initial analysis, we tested whether serum cholesterol levels effected WM microstructure (?<sup>1</sup>). Brain and serum cholesterol pools are largely independent, so we hypothesized that certain genes might exhibit pleiotropic effects on both serum and brain cholesterol pools and, thus, brain integrity. As cholesterol genes maintain serum cholesterol levels and AD genes influence brain structure, we analyzed the effects of a subset of cholesterol genes implicated in AD pathology on WM microstructure (?<sup>2</sup>). Abbreviations: AD, Alzheimer's disease; WM, white matter.

Each SNP was coded additively as 0, 1, or 2 according to the number of minor alleles present in each subject. The significance levels (*p*-value) of individual and joint SNP associations with FA, *D<sub>rad</sub>*, *D<sub>mean</sub>*, and *D<sub>ax</sub>* (radial, mean, and axial diffusivity; respectively) were determined from the *F*-score of the partial *F*-test:

$$F = \frac{\left( RSS_{\text{covariates}} - RSS_{\text{full}} \right) / \left( P_{\text{full}} - P_{\text{covariates}} \right)}{RSS_{\text{full}} / \left( n - P_{\text{full}} \right)} \quad (2)$$

Here, RSS represents the residual sum-of-squares (number of subjects, *n*). Our reduced model included only covariates (age, sex) as parameters (*P<sub>covariates</sub>*), and the full model contained all SNPs and covariates (*P<sub>full</sub>*). *p*-maps were generated for each individual SNP, covarying for each of the 17 other SNPs.

#### 2.6. Candidate gene analysis

As a post hoc test, we assessed the effect of the one SNP that contributed most to the multi-SNP results, examining its individual voxelwise associations with measures of microstructural WM integrity on the thresholded whole brain scans of QTIM participants. This test was not restricted to the CHOL mask generated earlier.

#### 2.7. Multiple comparisons correction

Computing multiple comparisons across thousands of voxels can introduce a high false-positive error rate (Genovese et al., 2002). To account for these errors, we used the searchlight false discovery rate (FDR) method to control the false positive rate of each statistical map at *q* = 0.05. Searchlight FDR controls for regional effects over FDR in any reported findings (Langner et al., 2007). All statistical maps shown in this article were thresholded at their corrected *p*-value after this multiple comparisons correction at *q* = 0.05 to show only regions of significance. Uncorrected *p*-values were then shown within the significant regions. When determining the

**Table 2**  
ADNI participants by probable diagnosis

	Probable diagnosis			
	AD	MCI	HC	Total
Participants	10	48	20	78
Men	6	31	12	49
Women	4	17	8	29
Average age at scan (y)	72.3 ± 11.4	74.4 ± 7.1	75.0 ± 5.4	74.3 ± 7.3

Average age (years at time of scan) and sex of ADNI participants, broken down by probable diagnosis.

Key: AD, Alzheimer's disease; ADNI, Alzheimer's disease neuroimaging initiative; HC, healthy controls; MCI, mild cognitive impairment.

significance of the effects of each individual SNP in the multi-SNP analysis (e.g., to identify our candidate SNP), we corrected for each of the 18 SNPs included in the joint analysis.

### 2.8. Follow-up analysis—ADNI cohort

To follow-up these findings, we also tested if there were any detectable associations in older participants from the ADNI. Our study included 78 participants (49 men and 29 women) with an average age of 74.3 ± 7.3 years. At the time of their baseline magnetic resonance imaging scan, each subject underwent multiple cognitive evaluations, including the Mini-Mental State Examination, Wechsler Memory Scale, Clinical Dementia Rating, and Alzheimer's Disease Assessment Scale-Cognitive, which were used to identify individuals as having AD or mild cognitive impairment (MCI), or they were classified as healthy controls (Nir et al., 2013). Definitive presence of AD pathology can only be confirmed via brain tissue biopsy or postmortem examination, so these diagnoses are only probable. Subject information for each probable diagnosis group is summarized in Table 2. Participants were scanned at one of 14 sites across North America. Inclusion and exclusion criteria are detailed in the ADNI protocol ([www.adni-info.org](http://www.adni-info.org)). All data from this cohort is publicly available at: <http://www.loni.usc.edu/ADNI/>.

The ADNI data set was chosen for use as an exploratory follow-up sample to study the candidate gene's associations with WM metrics in brain scans of older individuals, not because of the presence of AD and MCI diagnostic categories. As such, all probable diagnoses were included in the analysis to maximize our sample size, and probable disease status was covaried for, as AD is known to associate with measures of WM (Bartzokis et al., 2003; Parente et al., 2008; Rose et al., 2000).

ADNI was conducted according to Good Clinical Practice guidelines, the Declaration of Helsinki, US 21CFR Part 50—Protection of Human Subjects, and Part 56—Institutional Review Boards, and pursuant to state and federal HIPAA regulations. Written informed consent for the study was obtained from all participants and/or authorized representatives and study partners.

### 2.9. Follow-up analysis—statistical analysis

In our analysis, we covaried for sex, age, and probable disease status (using a dummy covariate for each of the diagnoses, AD and MCI) for our candidate SNP using the model listed in Equation 2. Candidate SNP allele dosage did not vary significantly between each probable diagnosis, and the allele frequency of each group was in Hardy-Weinberg equilibrium. APOE4 status is important to consider in elderly individuals when analyzing how cholesterol associated genes affect brain volume (Murphy et al., 2012). Thus, we ran additional analyses that covaried for APOE4 status. As only 57 participants had APOE4 information, we reran our initial analysis in this

smaller sub-sample, not covarying for APOE4, to eliminate group size effects. Demographic and genotypic information for both cohorts is summarized in Table 3.

### 2.10. DTI acquisition and processing

Images were acquired and processed as previously described (Jahanshad et al., 2012; Nir et al., 2013). Briefly, the following steps were performed: (1) images underwent distortion correction and intensive quality control; (2) DTI metrics were extracted from the tensor; (3) a study specific FA template was created to which we registered all individual FA maps; and (4) voxelwise associations were performed in regions of high FA in the template (FA >0.25 for healthy young adults and FA >0.2 for older ADNI participants). Additional details on image acquisition and processing and can be found in the Supplementary Methods section.

### 2.11. Explanation of DTI measures

A single diffusion tensor was fitted at each voxel in the brain from the eddy-current and Echo Planar Imaging (EPI) induced distortion corrected Diffusion Weighted Imaging (DWI) scans using the software package FMRIB Software Library (FSL), and scalar anisotropy and diffusivity measures were obtained from the resulting diffusion tensor eigenvalues including FA and radial, mean, and axial diffusivity ( $D_{\text{rad}}$ ,  $D_{\text{mean}}$ , and  $D_{\text{ax}}$ ).

Generally in healthy tissue, higher FA may indicate the presence of more heavily myelinated axons and is a well-accepted index of microstructural white matter integrity (Beaulieu, 2002; Klingberg et al., 2000). FA will therefore be high (nearer to 1) in regions of high organization (e.g., the corpus callosum), intermediate in regions with some organization (i.e., white matter regions with no predominant fiber orientation), low in regions that are not specifically oriented (i.e., gray matter), and near zero in free fluids (i.e., cerebrospinal fluid) (Grieve et al., 2007).

Lower FA can also indicate a reduction in the density of WM fibers, a loss in axonal bundle coherence, or a variation in membrane permeability to water (Beaulieu and Allen, 1994), so radial, mean, and axial diffusivity ( $D_{\text{rad}}$ ,  $D_{\text{mean}}$ ,  $D_{\text{ax}}$ ) are also commonly included

**Table 3**  
Participant demographic and genotypic information

	Database	
	QTIM	ADNI
Participants	403	78
Men	146	49
Women	257	29
Average age at scan (y)	23.8 ± 2.4	74.3 ± 7.3
Total cholesterol (mmol/L; mg/dL)	4.3 ± 0.7; 168 ± 28	NA
Low-density lipoproteins (mmol/L; mg/dL)	2.4 ± 0.6; 95 ± 24	NA
High-density lipoproteins (mmol/L; mg/dL)	1.4 ± 0.3; 54 ± 11	NA
Average age at cholesterol tests (y)	15.2 ± 2.3	NA
Number of cholesterol tests	2.2 ± 1.0	NA
rs5882 A/A	181	38
rs5882 A/G	185	32
rs5882 G/G	37	8
APOE4 homozygotes	NA	6
APOE4 heterozygotes	NA	19
APOE4 noncarriers	NA	32

Participant demographics for the QTIM and ADNI cohorts. For QTIM, we report mean total cholesterol (CHOL), high-density lipoproteins (HDL), and calculated low-density lipoproteins (LDL-c). Average serum cholesterol measures were within normal ranges for adolescents (CHOL <4.4 mmol/L [ $<170$  mg/dL]; HDL >0.9 mmol/L [ $>35$  mg/dL]; LDL <2.8 mmol/L [ $<110$  mg/dL]). In ADNI, APOE4 carrier status is included.

Key: ADNI, Alzheimer's disease neuroimaging initiative; NA, not applicable; QTIM, Queensland twin imaging.

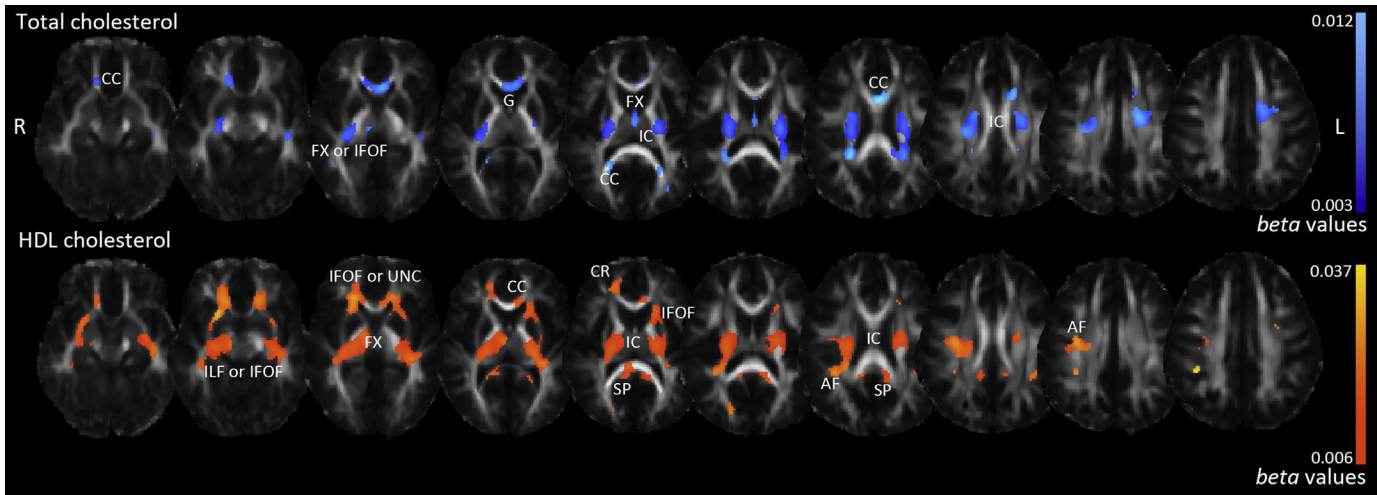


**Fig. 2.** Associations between white matter microstructure (FA) and total cholesterol (CHOL) and high-density lipoprotein (HDL) in the QTIM sample. Higher adolescent serum levels of both CHOL and HDL were associated with higher FA in early adulthood. For total cholesterol, light blue areas correspond to stronger beta-values (regression coefficients more positive); for high-density lipoprotein, yellow areas correspond to stronger beta-values (more positive). Both measures positively associate with FA but are represented in different colors to capture the specific beta-value ranges for each test. Abbreviations: AF, arcuate fasciculus; CC, corpus callosum; CR, corona radiata; FA, fractional anisotropy; FX, fornix; G, genu; IC, internal capsule; IFOF, inferior fronto-occipital fasciculus; ILF, inferior longitudinal fasciculus; SP, splenium; QTIM, Queensland twin imaging; UNC, uncinate. Left in the image is right in the brain. (For interpretation of the references to color in this figure, the reader is referred to the web version of this article.)

in WM assessments (Barysheva et al., 2013).  $D_{\text{ax}}$  ( $\lambda_1$ ) represents the tendency of water to diffuse along its primary direction of diffusion.  $D_{\text{rad}}$  (the average of  $\lambda_2$  and  $\lambda_3$ ) measures diffusion perpendicular to the axonal fibers.  $D_{\text{rad}}$  is thought to be minimally affected by the loss of bundle coherence and often increases when myelin is damaged or fails to develop normally (Song et al., 2002, 2005; Thomason and Thompson, 2011).  $D_{\text{mean}}$  ( $\hat{\lambda}$ ) is the average of the diffusivities in the 3 principal diffusion directions. Thus,  $D_{\text{mean}}$  provides an overall evaluation of the molecular motion in a voxel or region, characterizing the overall presence of obstacles to diffusion (Thomason and Thompson, 2011). The combined use of these diffusivity measures gives a clearer picture of WM microstructure.

### 3. Results

#### 3.1. Cholesterol analysis

Serum cholesterol concentrations and DTI images were available for 403 individuals from the QTIM cohort (see Demographics, Table 3). We mapped the voxelwise effects of averaged adolescent blood serum cholesterol measures (CHOL, HDL, and LDL-c; average collection age = 15.2 years) across the thresholded WM regions of the whole brain to determine associations with white matter integrity. Higher CHOL was associated (after multiple comparisons correction as described in the Methods) with higher FA across broad regions of white matter, including the genu of the corpus callosum (G), corpus callosum overall (CC), fornix (FX), internal capsule (IC), and the inferior fronto-occipital fasciculus (IFOF) (Fig. 2). Furthermore, higher CHOL was associated with lower  $D_{\text{rad}}$ ,  $D_{\text{mean}}$ , and  $D_{\text{ax}}$  (with negative beta-values) (Supplementary Fig. 1).

Higher HDL was associated with higher FA in the splenium of the corpus callosum (SP), the IC, arcuate fasciculus (AF), FX, CC, corona radiata (CR), and regions corresponding to the IFOF, inferior longitudinal fasciculus (ILF), and/or uncinate (UNC) (Fig. 2). Higher HDL was associated with lower  $D_{\text{rad}}$  (Supplementary Fig. 2), but variation in HDL was not significantly associated with  $D_{\text{ax}}$  and  $D_{\text{mean}}$ . LDL-c was not significantly associated with FA; thus, other measures of WM microstructure ( $D_{\text{ax}}$ ,  $D_{\text{rad}}$ , and  $D_{\text{mean}}$ ) were not further investigated.

#### 3.2. Multi-SNP analysis

As adolescent CHOL levels were associated with WM structure in adulthood, we further examined common variants in a subset of cholesterol-related genes previously associated with AD risk (Table 1). Using a multi-SNP genetic model (Kohannim et al., 2012), we examined the joint effect of allele dosage of 18 SNPs on brain regions where CHOL was associated with FA. This avoided correction across unnecessary tests at potentially unrelated voxels or voxels with poor signal-to-noise ratio and boosted detection sensitivity by limiting the search space.

The multi-SNP analysis shows the proportion of variance ( $R^2$ ) in FA explained by our SNP panel. Significant predictions of FA were made by the joint multi-SNP model ( $p$ -value =  $1.09 \times 10^{-5}$ , critical  $p$ -value of 0.023 in 46.7% of voxels of the CHOL FA mask in the IC, CC, and the IFOF and/or ILF (Fig. 3). The critical  $p$ -value is the highest threshold that controls the FDR, and higher critical  $p$ -values (closer to 0.05) denote stronger effects.

We generated  $p$ -maps for the individual associations with FA for each SNP, simultaneously covarying for the effects of the other SNPs. rs5882 of *CETP* individually survived multiple comparisons correction across all voxels using FDR at  $q = 0.05$  individually (minimum voxelwise  $p$ -value =  $6.54 \times 10^{-7}$ , critical  $p$ -value = 0.033). For the main multi-SNP analysis, only 1 statistical test is completed so no further correction is necessary for the number of SNPs in the analysis. For the individual SNP analyses, however, we corrected for both the number of voxels tested and the number of SNPs tested. Even so, rs5882 in *CETP* was statistically significant at the new more stringent significance threshold ( $p$ -value =  $7.61 \times 10^{-7}$ ).

#### 3.3. Candidate gene analyses

After identifying candidate gene *CETP* (rs5882) from the multi-SNP analysis, we performed individual voxelwise examinations of rs5882 G-allele dosage on thresholded FA,  $D_{\text{ax}}$ ,  $D_{\text{mean}}$ , and  $D_{\text{rad}}$  maps of the entire brain (not restricted to the areas associated with CHOL). In the QTIM sample (young healthy adults), increased rs5882 risk (G) allele dosage was significantly associated with

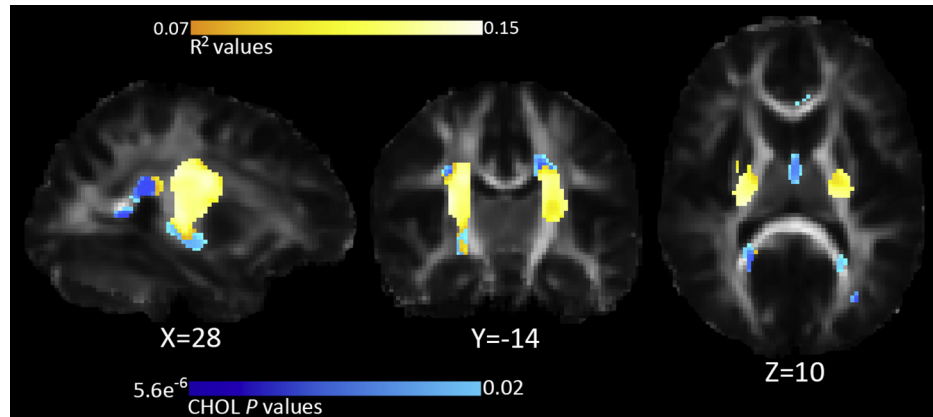


**Fig. 3.** Multi-SNP results:  $R^2$  values for significant associations of the multi-SNP analysis within brain regions associated with total cholesterol in the QTIM sample.  $R^2$  values are combined predictive value of our SNPs. White areas are areas with higher  $R^2$  values, as shown by the color bar. The blue underlay corresponds to the  $p$ -values of the CHOL analysis; these were used to define a search region for the multi-SNP analysis. Thus, blue regions visible represent the only regions of the CHOL FA mask where the multi-SNP analysis did not find significant associations. Left in the image is right in the brain, coordinates are in MNI space. Abbreviations: CHOL, total cholesterol; FA, fractional anisotropy; SNP, single-nucleotide polymorphism; QTIM, Queensland twin imaging. (For interpretation of the references to color in this figure, the reader is referred to the web version of this article.)

higher FA (minimum voxelwise  $p$ -value =  $9.47 \times 10^{-8}$ , critical  $p$ -value = 0.019) bilaterally in the internal capsule (IC), splenium of the corpus callosum (SP), arcuate fasciculus (AF), and areas corresponding to the uncinate (UNC), inferior longitudinal fasciculus (ILF), and/or inferior fronto-occipital fasciculus (IFOF) (Fig. 4A). Higher rs5882 risk allele dosage was also associated with lower  $D_{rad}$  and  $D_{mean}$  (Supplementary Fig. 3).

#### 3.4. Follow-up analysis in ADNI

As rs5882 showed broad associations in the white matter tracts of healthy young adults (QTIM; mean age 23.8 years, SD = 2.4), we searched for effects of this SNP in late life by analyzing rs5882 allele-dosage dependent voxelwise associations with measures of WM over the whole thresholded brain images in ADNI (mean age 74.3 years, SD = 7.3). Risk (G) allele dosage of rs5882 was associated with lower FA ( $p$ -value =  $4.53 \times 10^{-6}$ , critical  $p$ -value = 0.0019) in the IFG, CC (forceps major), SP, CR, and regions corresponding to the ILF, IFOF, UNC, and/or FX (Fig. 4B). This pattern was directionally opposite of our QTIM findings, but agrees with prior reports that A-allele dosage is associated with greater baseline thickness and less atrophy in elderly APOE4 noncarriers (Murphy et al., 2012). rs5882 risk allele dosage was also associated with higher  $D_{rad}$  and  $D_{mean}$  (Supplementary Fig. 4). CETP and APOE interact (Arias-Vasquez et al., 2007; Murphy et al., 2012), so we also ran the analysis covarying for APOE status. rs5882 risk allele dosage continued to show negative associations with FA.

## 4. Discussion

In this study, we set out to further our understanding of the relationship between cholesterol, genetics, and the brain in young and old individuals. We found significant associations between elevated total adolescent cholesterol (CHOL) and HDL levels and higher FA measured from DTI images acquired during early adulthood (QTIM). Ensuing analyses with other diffusivity measures suggested that higher cholesterol levels are indeed associated with greater WM integrity. We also found that cholesterol genes were associated with FA in these young adults in regions with substantial overlap to serum cholesterol measures. One SNP, rs5882 of CETP, independently held significant associations with DTI metrics, showing differential effects in younger (QTIM) and older populations (ADNI).

Changes in magnetic resonance imaging signal, as detected by fractional anisotropy, can be attributed to a number of physiological factors including edema, demyelination, and inflammation (Assaf and Pasternak, 2008; Thomason and Thompson, 2011). The different processes contributing to significant signal change can potentially be distinguished by investigating the different diffusivity maps generated in DTI studies (Assaf and Pasternak, 2008). We performed our analyses with multiple DTI-derived measures (fractional anisotropy and axial, radial, and mean diffusivities) to provide a clearer picture of the white matter microstructural differences identified. Some of these metrics have been studied in post-mortem analyses and animal model studies, and  $D_{rad}$  has potentially shown specificity for assessment of myelination (Song et al., 2005). For a full explanation of DTI-derived measures, see Section 2.

In voxel-based analyses, the presence of gray matter, white matter, and cerebrospinal fluid within a single voxel lead to partial voluming (Lee et al., 2009). This effect is amplified in scans acquired with larger slice thicknesses or greater voxel size. By limiting our statistical tests to regions where the template showed an FA > 0.25 (0.2 for the older cohort), we attempted to limit our analyses to highly probable white matter voxels where partial voluming plays a minimal role. However, because of voxel sizes much larger than axonal bundles, partial voluming remains an inherent limitation in current DTI analyses.

The bulk of cholesterol biosynthesis during brain maturation is produced for myelin development (Morell and Jurevics, 1996) and myelination continues well into adulthood. Only recently has imaging been used to examine associations between serum cholesterol levels and brain structure *in vivo*. To our knowledge, our article is the first to examine such associations in young adults. Elevated CHOL and HDL measured during adolescence were associated with greater FA levels and, more specifically, lower  $D_{rad}$  in young adults. Higher cholesterol levels in early life may be associated with more robust myelination and greater progression along the WM developmental trajectory, contributing to greater WM microstructural integrity. Cholesterol analyses were only performed on the QTIM data set.

Serum cholesterol levels increase nearly linearly from adolescence through mid-life at an annual rate of 2.29 mg/dL (0.06 mmol/L) (Keys et al., 1950). As all QTIM participants were healthy, little deviation from this trend is expected. Because of the linear relationship, durations between serum collection (average age  $15.2 \pm 2.3$  years) and scan time will be almost exclusively correlated with

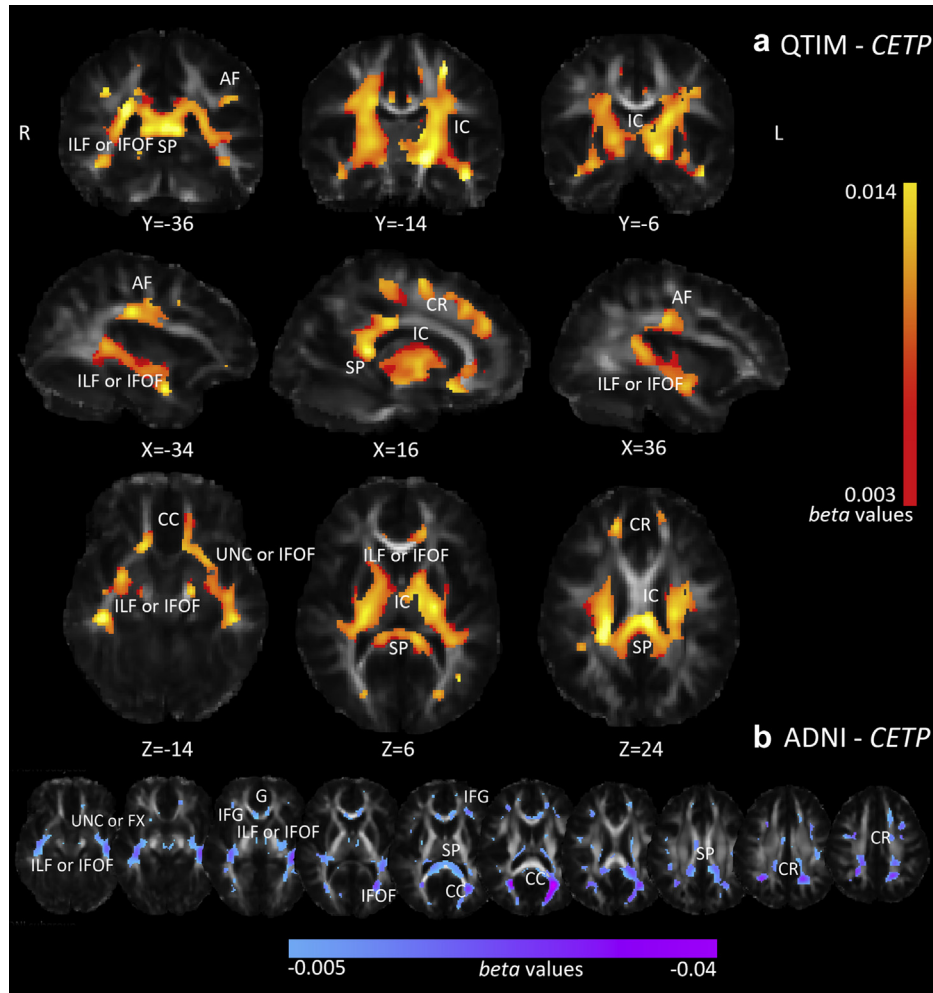


**Fig. 4.** Significant associations between white matter microstructure (as measured here by thresholded whole brain voxel-wise FA) and CETP (rs5882) risk (G) allele dosage in (A) the QTIM sample and (B) ADNI. In QTIM (A), increased G-allele dosage was associated with higher FA in statistically significant regions. Yellow corresponds to stronger beta-values (more positive). In ADNI (B), increased G-allele dosage was associated with lower FA in statistically significant regions. Pink corresponds to stronger beta-values (more negative). Only areas surviving multiple comparisons correction across the brain are shown. Abbreviations: ADNI, Alzheimer's disease neuroimaging initiative; AF, arcuate fasciculus; CC, corpus callosum; CR, corona radiata; FA, fractional anisotropy; FDR, false discovery rate; FX, fornix; G, genu; IC, internal capsule; IFG, inferior frontal gyrus; IFOF, inferior fronto-occipital fasciculus; ILF, inferior longitudinal fasciculus; SP, splenium; QTIM, Queensland twin imaging; UNC, uncinate. Left in the image is right in the brain, coordinates are in MNI space. (For interpretation of the references to color in this figure, the reader is referred to the web version of this article.)

age at the time of the scan (average age  $23.8 \pm 2.0$  years) and therefore are not modeled separately.

Although statistically significant associations between CHOL/HDL and FA were detected in broad WM regions in the young adults, cholesterol may simply have a more generalized effect on WM throughout the brain. Associations between cholesterol levels and FA are conventionally shown for regions where the estimated effect size for a set of voxels exceeds that expected by chance (searchlight FDR thresholded at  $q = 0.05$ ). Thus, any inference about where the association is detected does not imply that the effects are not present elsewhere in the brain (Jernigan et al., 2003). Lack of standardization in the brain's arterial supply (Tatu et al., 1996), differences in age of maturation of different white matter regions (Tamnes et al., 2010), and other anatomic variability may, in part, contribute to the detectability of a statistical association in any brain region.

Cholesterol concentration is influenced by genetics, so we performed a voxelwise joint multi-SNP analysis on brain regions significantly associated with CHOL in the young adults. Several AD risk genes overlap with those that may increase a person's risk for high

serum cholesterol (Arias-Vasquez et al., 2007; Rodriguez-Rodriguez et al., 2009; Solfrizzi et al., 2002; Wollmer et al., 2003). AD pathology is marked by a global cognitive decline (Moseley, 2002) and by alterations in various WM structures of the brain (Bartzokis et al., 2003; Bozzali et al., 2002; Brun and Englund, 1986; Rose et al., 2000), with lower FA observed in AD patients versus healthy controls (Parente et al., 2008; Rose et al., 2008; Takahashi et al., 2002). DTI metrics have even detected changes in the WM microstructure between healthy elderly individuals and patients with MCI (Bosch et al., 2012; Ukmarr et al., 2008), indicating the usage of mapping the effects of risk-variants before the onset of disease. As thousands of SNPs are implicated in the cholesterol metabolizing pathway, we narrowed our search to a panel of 18 cholesterol related SNPs previously associated with AD risk, which have known neurologic involvement. Significant associations were detected between this set of genes and FA, suggesting that variations in the cholesterol-metabolizing pathway influence WM microstructure. These genes may affect the local concentration of cholesterol available to oligodendrocytes, as CNS myelination is hindered when cholesterol synthesis is impaired in oligodendrocytes (Saher et al., 2005).

The multi-SNP analysis also identified the variant of the cholesterol-related genes with the largest influence on FA, *CETP* (rs5582). The role of *CETP* (cholesteryl ester transfer protein) in plasma has been extensively studied (Ruggeri, 2005), but its role in the brain is less well understood. *CETP* protein product is detectable in cerebrospinal fluid (Tall, 1993), suggesting that the gene influences the cholesterol concentration available to the brain. *CETP* mediates transfer of cholesteryl esters from HDL to LDL and other lipoproteins and promotes subsequent uptake by the cell (Inazu et al., 1990). *CETP* rs5582 (I405V) represents an A to G variation, which encodes valine in place of isoleucine. Risk (G) allele homozygotes show significantly lower *CETP* and higher HDL levels (Arias-Vasquez et al., 2007; Asselbergs et al., 2012).

In young adults, the rs5582 risk-allele dosage, assessed additively, was broadly associated with higher FA: risk (G-allele) homozygotes had higher FA than A-allele homozygotes and heterozygotes. Significantly lower radial diffusivity and mean diffusivity were also observed with increasing risk-allele dosage. Thus, the rs5582 I405V variant may lead to greater myelination and axonal integrity during brain development. As higher cholesterol levels are essential for maturation, abundant or elevated HDL levels may serve a critical role in the development of heavily myelinated white matter fibers.

Turley et al. (1996) suggest that LDL cholesterol plays little to no role in the sterol acquiring process of the developing brain, and, in our own analysis, LDL-c failed to show significant associations with DTI correlates of white matter microstructure in young adults.

Although elevated cholesterol levels may support brain development, higher cholesterol later in life may be detrimental to the brain. In addition to increasing risk for degenerative brain disease (Refolo et al., 2000), hypercholesterolemia also contributes to higher risk for developing cerebrovascular disorders (Kaste and Koivisto, 1988), including dysfunction of the blood brain barrier (Kalayci et al., 2009). Prior studies have found negative associations between serum cholesterol measures and FA in older individuals (Cohen et al., 2011; Williams et al., 2013) (average age of participants =  $58.3 \pm 1.2$  and  $68.0 \pm 9.4$  years, respectively). As Cohen et al. (2011) jointly analyzed the effects of “abnormal cholesterol” (high HDL, low LDL, and/or statin use), we cannot directly relate our findings to their results. Contrary to results from our younger cohort, Williams et al. (2013) reported that greater HDL was associated with lower FA in an older group. Although serum cholesterol information was not available for all older participants evaluated from ADNI, we found that rs5582 risk-allele dosage (associated with higher HDL, Asselbergs et al., 2012) was associated with lower FA and higher  $D_{rad}$  and  $D_{mean}$ , suggesting lower WM microstructural integrity. Here, higher  $D_{rad}$  may be indicative of lower levels of myelination.

Some WM regions where FA associations with serum cholesterol levels were detected (genu of the corpus callosum, inferior longitudinal fasciculus) are among the earliest and most rapidly changing WM tracts (Lebel et al., 2008), suggesting that WM microstructure in these areas may be more susceptible to cholesterol concentration present during the crucial developmental period. Although many different models describe the underlying association between WM and AD (Bartzokis, 2011; Nir et al., 2013), WM atrophy is often attributed, in part, to Wallerian degeneration and therefore may be secondary to gray matter loss (Bozzali et al., 2002). Axonal integrity of the splenium of the corpus callosum (SP), among other regions, is lower in AD patients (Chua et al., 2008). Associations between cholesterol-gene *CETP* risk-allele dosage and WM were found in the SP of young, healthy adults, suggesting that there may be a genetic component influencing these changes long before the onset of disease or age-

related degeneration. Validation of our findings and proof of differential effects across brain regions would require a more focused study of cholesterol throughout development or a longitudinal assessment of cognitive impairment, which are beyond the scope of this study.

In summary, although previous studies have shown associations between serum cholesterol levels and brain structure in older adults, this study may be the first to suggest that higher cholesterol levels are associated with greater white matter microstructural integrity in young adults. Cholesterol-related genetic variants predicted FA in nearly half of these WM regions associated with serum cholesterol. As serum cholesterol is essentially separated from brain cholesterol, these genes may also act in the brain to affect the local cholesterol microenvironment and, as a result, WM integrity. rs5582 risk (G) allele dosage showed opposite directional associations in 2 groups of participants most likely because of age differences between the cohorts, predicting significantly higher WM integrity in young adults and lower WM integrity in old adults. Because this specific variant forms a gene product that promotes elevated HDL, high HDL may be beneficial during WM development and detrimental later in life. Additional studies are needed to provide further evidence that the association is not a false positive.

The relationship between cholesterol and the brain is important for understanding the healthy aging process and pathology. When cholesterol available to the brain is reduced during development, white matter maturation is significantly affected. Lower white matter integrity could lead to slower signaling and impaired cognitive function, specifically in tasks requiring rapid decision and movement times (Muldoon et al., 1997). Late-life hypercholesterolemia, by contrast, is associated with cognitive decline (Elias et al., 2005; Solomon et al., 2009) and higher risk for late-onset AD in several studies (Reid et al., 2007; Sparks, 1997). Optimal cholesterol levels in the brain change over the life span, so some cholesterol-related genetic variations may be beneficial to white matter microstructural integrity early in life and detrimental later. Future longitudinal research is required to further elucidate how the favorable range of cholesterol levels changes throughout life and how these changes affect the brain. Study of the detrimental effects of unfavorable cholesterol levels may help us understand genetic risk decades before disease onset and may even lead to the development of novel therapeutic targets.

## Disclosure statement

The authors have no competing financial interests.

## Acknowledgements

This study was supported by the National Institute of Child Health and Human Development (R01 HD050735), and the National Health and Medical Research Council (486682, 1009064), Australia. Genotyping was supported by National Health and Medical Research Council (389875). Additional support for algorithm development was provided by National Institutes of Health R01 grants EB008432, EB008281, EB007813, P41RR013642, and 5R01MH094343. Emily L. Dennis was funded, in part, by an National Institutes of Health Training Grant in Neurobehavioral Genetics (T32 MH073526-06). The Alzheimer's Disease Neuro-imaging Initiative (ADNI) was supported by public and private funding sources, found at (<http://www.adni-info.org/Scientists/ADNISponsorsAndPartners.aspx>).

## Appendix A. Supplementary data

Supplementary data associated with this article can be found, in the online version, at <http://dx.doi.org/10.1016/j.neurobiolaging.2014.05.024>.

## References

- Annett, M., 1970. A classification of hand preference by association analysis. *Br. J. Psychol.* 61, 303–321.
- Arias-Vasquez, A., Isaacs, A., Aulchenko, Y.S., Hofman, A., Oostra, B.A., Breteler, M., van Duijn, C.M., 2007. The cholesteryl ester transfer protein (CETP) gene and the risk of Alzheimer's disease. *Neurogenetics* 8, 189–193.
- Assaf, Y., Pasternak, O., 2008. Diffusion tensor imaging (DTI)-based white matter mapping in brain research: a review. *J. Mol. Neurosci.* 34, 51–61.
- Asselbergs, F.W., Guo, Y., van Iperen, E.P., Sivapalaratnam, S., Tragante, V., Lanktree, M.B., Lange, L.A., Almoguera, B., Appelman, Y.E., Barnard, J., Baumert, J., Beitelshees, A.L., Bhangale, T.R., Chen, Y.I., Gaunt, T.R., Gong, Y., Hopewell, J.C., Johnson, T., Kleber, M.E., Langaee, T.Y., Li, M., Li, Y.R., Liu, K., McDonough, C.W., Meijis, M.F.L., Middelberg, R.P.S., Musunuru, K., Nelson, C.P., O'Connell, J.R., Padmanabhan, S., Pankow, J.S., Pankratz, N., Rafelt, S., Rajagopalan, R., Romaine, S.P.R., Schork, N.J., Shaffer, J., Shen, H., Smith, E.N., Tischfield, S.E., van Vliet-Ostaptchouk, J.V., Verweij, N., Volcik, K.A., Zhang, L., Bailey, K.R., Bailey, K.M., Bauer, F., Boer, J.M.A., Braund, P.S., Burt, A., Burton, P.R., Buxbaum, S.G., Chen, W., Cooper-Dehoff, R.M., Cupples, L.A., DeJong, J.S., Delles, C., Duggan, D., Fornage, M., Furlong, C.E., Glazer, N., Gums, J.G., Hastie, C., Holmes, M.V., Illig, T., Kirkland, S.A., Kivimaki, M., Klein, R., Klein, B.E., Kooperberg, C., Kottke-Marchant, K., Kumari, M., LaCroix, A.Z., Mallela, L., Murugesan, G., Ordovas, J., Ouwehand, W.H., Post, W.S., Saxena, R., Scharnagl, H., Schreiner, P.J., Shah, T., Shields, D.C., Shimbo, D., Srinivasan, S.R., Stolk, R.P., Swerdlow, D.L., Taylor, H.A., Topol, E.J., Toskala, E., van Pelt, J.L., van Setten, J., Yusuf, S., Whittaker, J.C., Zwinderman, A.H., Anand, S.S., Balmforth, A.J., Berenson, G.S., Bezzina, C.R., Boehm, B.O., Boerwinkle, E., Casas, J.P., Caulfield, M.J., Clarke, R., Connell, J.M., Cruickshanks, K.J., Davidson, K.W., Day, I.N.M., de Bakker, P.I.W., Doevendans, P.A., Dominicak, A.F., Hall, A.S., Hartman, C.A., Hengstenberg, C., Hillege, H.L., Hofker, M.H., Humphries, S.E., Jarvik, G.P., Johnson, J.A., Kaess, B.M., Kathiresan, S., Koenig, W., Lawlor, D.A., März, W., Melander, O., Mitchell, B.D., Montgomery, G.W., Munroe, P.B., Murray, S.S., Newhouse, S.J., Onland-Moret, N.C., Poulter, N., Psaty, B., Redline, S., Rich, S.S., Rotter, J.I., Schunkert, H., Sever, P., Shuldiner, A.R., Silverstein, R.L., Stanton, A., Thorand, B., Trip, M.D., Tsai, M.Y., van der Harst, P., van der Schoot, E., van der Schouw, Y.T., Verschuren, W.M.M., Watkins, H., Wilde, A.A.M., Wolffenbuttel, B.H.R., Whitfield, J.B., Hovingh, G.K., Ballantyne, C.M., Wijmenga, C., Reilly, M.P., Martin, N.G., Wilson, J.G., Rader, D.J., Samani, N.J., Reiner, A.P., Hegele, R.A., Kastelein, J.J.P., Hingorani, A.D., Talmud, P.J., Hakonarson, H., Elbers, C.C., Keating, B.J., Drenos, F., 2012. Large-scale genome-wide meta-analysis across 32 studies identifies multiple lipid loci. *Am. J. Hum. Genet.* 91, 823–838.
- Asselbergs, F.W., Lovering, R.C., Drenos, F., 2013. Progress in genetic association studies of plasma lipids. *Curr. Opin. Lipidol.* 24, 123–128.
- Astarita, G., Jung, K.M., Berchtold, N.C., Nguyen, V.Q., Gillen, D.L., Head, E., Cotman, C.W., Piomelli, D., 2010. Deficient liver biosynthesis of docosahexaenoic acid correlates with cognitive impairment in Alzheimer's disease. *PLoS One* 5, e12538. *PLoS One* 5, e12538.
- Aukema, E.J., Caan, M.W., Oudhuis, N., Majoie, C.B., Vos, F.M., Reneman, L., Last, B.F., Grootenhuis, M.A., Schouten-van Meeteren, A.Y.N., 2009. White matter fractional anisotropy correlates with speed of processing and motor speed in young childhood cancer survivors. *Int. J. Radiat. Oncol. Biol. Phys.* 74, 837–843.
- Bartzokis, G., 2011. Alzheimer's disease as homeostatic responses to age-related myelin breakdown. *Neurobiol. Aging* 32, 1341–1371.
- Bartzokis, G., Cummings, J.L., Sultzter, D., Henderson, V.W., Nuechterlein, K.H., Mintz, J., 2003. White matter structural integrity in healthy aging adults and patients with Alzheimer disease: a magnetic resonance imaging study. *Arch. Neurol.* 60, 393–398.
- Bartzokis, G., Sultzter, D., Lu, P.H., Nuechterlein, K.H., Mintz, J., Cummings, J.L., 2004. Heterogeneous age-related breakdown of white matter structural integrity: implications for cortical "disconnection" in aging and Alzheimer's disease. *Neurobiol. Aging* 25, 843–851.
- Barysheva, M., Jahanshad, N., Foland-Ross, L., Altshuler, L.L., Thompson, P.M., 2013. White matter microstructural abnormalities in bipolar disorder: a whole brain diffusion tensor imaging study. *Neuroimage Clin.* 2, 558–568.
- Baum, L., Chen, L., Masliah, E., Chan, Y.S., Ng, H.K., Pang, C.P., 1999. Lipoprotein lipase mutations and Alzheimer's disease. *Am. J. Med. Genet.* 88, 136–139.
- Beaulieu, C., 2002. The basis of anisotropic water diffusion in the nervous system - a technical review. *NMR Biomed.* 15, 435–455.
- Beaulieu, C., Allen, P.S., 1994. Water diffusion in the giant axon of the squid: implications for diffusion-weighted MRI of the nervous system. *Magn. Reson. Med.* 32, 579–583.
- Benton, D., 1995. Do low cholesterol levels slow mental processing? *Psychosom. Med.* 57, 50–53.
- Bosch, B., Arenaza-Urquijo, E.M., Rami, L., Sala-Llonch, R., Junqué, C., Solé-Padullés, C., Bartrés-Faz, D., 2012. Multiple DTI index analysis in normal aging, amnestic MCI and AD. Relationship with neuropsychological performance. *Neurobiol. Aging* 33, 61–74.
- Bozzali, M., Falini, A., Franceschi, M., Cercignani, M., Zuffi, M., Scotti, G., Comi, G., Filippi, M., 2002. White matter damage in Alzheimer's disease assessed in vivo using diffusion tensor magnetic resonance imaging. *J. Neurol. Neurosurg. Psychiatry* 72, 742–746.
- Brun, A., Englund, E., 1986. A white matter disorder in dementia of the Alzheimer type: a pathoanatomical study. *Ann. Neurol.* 19, 253–262.
- Chiang, M.C., Barysheva, M., Shattuck, D.W., Lee, A.D., Madsen, S.K., Avedissian, C., Klunder, A.D., Toga, A.W., McMahon, K.L., de Zubicaray, G.I., Wright, M.J., Srivastava, A., Balov, N., Thompson, P.M., 2009. Genetics of brain fiber architecture and intellectual performance. *J. Neurosci.* 29, 2212–2224.
- Chua, T.C., Wen, W., Slavin, M.J., Sachdev, P.S., 2008. Diffusion tensor imaging in mild cognitive impairment and Alzheimer's disease: a review. *Curr. Opin. Neurol.* 21, 83–92.
- Cohen, J.I., Cazettes, F., Convit, A., 2011. Abnormal cholesterol is associated with prefrontal white matter abnormalities among obese adults, a diffusion tensor imaging study. *Neuroradiol. J.* 1 (21), 989.
- Deroesne, C., Thibault, S., Lagha-Pierucci, S., Baudouin-Madec, V., Ancri, D., Lacromblez, L., 1999. Decreased awareness of cognitive deficits in patients with mild dementia of the Alzheimer type. *Int. J. Geriatr. Psychiatry* 14, 1019–1030.
- Dietschy, J.M., Turley, S.D., 2004. Thematic review series: brain lipids. Cholesterol metabolism in the central nervous system during early development and in the mature animal. *J. Lipid Res.* 45, 1375–1397.
- Dzamko, N., Alessi, D.R., Birk, O.S., 2011. Enzyme may be responsible for regulating deleterious effects of Alzheimer's disease in the brain. *Future Neurol.* 6, 9–11.
- Elias, P.K., Elias, M.F., D'Agostino, R.B., Sullivan, L.M., Wolf, P.A., 2005. Serum cholesterol and cognitive performance in the Framingham Heart Study. *Psychosom. Med.* 67, 24–30.
- Genovese, C.R., Lazar, N.A., Nichols, T., 2002. Thresholding of statistical maps in functional neuroimaging using the false discovery rate. *Neuroimage* 15 (4), 870–878.
- Grieve, S.M., Williams, L.M., Paul, R.H., Clark, C.R., Gordon, E., 2007. Cognitive aging, executive function, and fractional anisotropy: a diffusion tensor MR imaging study. *AJNR Am. J. Neuroradiol.* 28, 226–235.
- Gustafson, C., Glerup, S., Pallesen, L.T., Olsen, D., Andersen, O.M., Nykjaer, A., Madsen, P., Petersen, C.M., 2013. Sortilin and SorLA display distinct roles in processing and trafficking of amyloid precursor protein. *J. Neurosci.* 33, 64–71.
- Hüppi, P.S., Dubois, J., 2006. Diffusion tensor imaging of brain development. *Semin. Fetal Neonatal Med.* 11 (6), 489–497.
- Ikeda, T., Yamada, M., 2010. [Risk factors for Alzheimer's disease]. *Brain Nerve* 62, 679–690.
- Inazu, A., Brown, M.L., Hesler, C.B., Agellon, L.B., Koizumi, J., Takata, K., Maruhama, Y., Mabuchi, H., Tall, A.R., 1990. Increased high-density lipoprotein levels caused by a common cholesteryl-ester transfer protein gene mutation. *N. Engl. J. Med.* 323, 1234–1238.
- Jahanshad, N., Kochunov, P.V., Sprooten, E., Mandl, R.C., Nichols, T.E., Almasy, L., Blangero, J., Brouwer, R.M., Curran, J.E., de Zubicaray, G.I., Duggirala, R., Fox, P.T., Hong, L.E., Landman, B.A., Martin, N.G., McMahon, K.L., Medland, S.E., Mitchell, B.D., Olvera, R.L., Peterson, C.P., Starro, J.M., Sussmann, J.E., Toga, A.W., Wardlaw, J.M., Wright, M.J., Hulshoff Pol, H.E., Bastin, M.E., McIntosh, A.M., Deary, I.J., Thompson, P.M., Glahn, D.C., 2013. Multi-site genetic analysis of diffusion images and voxelwise heritability analysis: a pilot project of the ENIGMA-DTI working group. *Neuroimage* 81, 455–469.
- Jahanshad, N., Kohannim, O., Hibar, D.P., Stein, J.L., McMahon, K.L., de Zubicaray, G.I., Medland, S.E., Montgomery, G.W., Whitfield, J.B., Martin, N.G., Wright, M.J., Toga, A.W., Thompson, P.M., 2012. Brain structure in healthy adults is related to serum transferrin and the H63D polymorphism in the HFE gene. *Proc. Natl. Acad. Sci. U.S.A.* 109, E851–E859.
- Jernigan, T.L., Gamst, A.C., Fennema-Notestine, C., Ostergaard, A.L., 2003. More "mapping" in brain mapping: statistical comparison of effects. *Hum. Brain Mapp.* 19, 90–95.
- Jin, Y., Shi, Y., Joshi, S.H., Jahanshad, N., Zhan, L., De Zubicaray, G.I., Thompson, P.M., 2010. Heritability of white matter fiber tract shapes: a HARDI study of 198 twins. In: *Multimodal Brain Image Analysis* (pp. 35–43). Held in Conjunction with MICCAI 2011, Toronto, Canada.
- Kalayci, R., Kaya, M., Uzun, H., Bilgic, B., Ahishali, B., Arican, N., Elmaz, I., Küçük, M., 2009. Influence of hypercholesterolemia and hypertension on the integrity of the blood-brain barrier in rats. *Int. J. Neurosci.* 119, 1881–1904.
- Kang, H.M., Zaitlen, N.A., Wade, C.M., Kirby, A., Heckerman, D., Daly, M.J., Eskin, E., 2008. Efficient control of population structure in model organism association mapping. *Genetics* 178, 1709–1723.
- Kaste, M., Koivisto, P., 1988. Risk of brain infarction in familial hypercholesterolemia. *Stroke* 19, 1097–1100.
- Keys, A., Mickelsen, O., Miller, E.V., Hayes, E.R., Todd, R.L., 1950. The concentration of cholesterol in the blood serum of normal man and its relation to age. *J. Clin. Invest.* 29, 1347.
- Klingberg, T., Hedeus, M., Temple, E., Salz, T., Gabrieli, J.D., Moseley, M.E., Poldrack, R.A., 2000. Microstructure of temporo-parietal white matter as a basis for reading ability: evidence from diffusion tensor magnetic resonance imaging. *Neuron* 25, 493–500.
- Kochunov, P., Coyle, T., Lancaster, J., Robin, D.A., Hardies, J., Kochunov, V., Bartzokis, G., Stanley, J., Royall, D., Schlosser, A.E., Null, M., Fox, P.T., 2010. Processing speed is correlated with cerebral health markers in the frontal lobes as quantified by neuroimaging. *Neuroimage* 49, 1190–1199.

- Kohannim, O., Jahanshad, N., Braskie, M.N., Stein, J.L., Chiang, M.C., Reese, A.H., Hibar, D.P., Toga, A.W., McMahon, K.L., de Zubicaray, G.I., Medland, S.E., Montgomery, G.W., Martin, N.G., Wright, M.J., Thompson, P.M., 2012. Predicting white matter integrity from multiple common genetic variants. *Neuro-psychopharmacology* 37, 2012–2019.
- Kysenius, K., Muggalla, P., Matlik, K., Arumae, U., Huttunen, H.J., 2012. PCSK9 regulates neuronal apoptosis by adjusting ApoER2 levels and signaling. *Cell Mol. Life Sci.* 69, 1903–1916.
- Lamsa, R., Helisalmi, S., Herukka, S.K., Tapiola, T., Pirttila, T., Vepsäläinen, S., Hiltunen, M., Soininen, H., 2008. Genetic study evaluating LDLR polymorphisms and Alzheimer's disease. *Neurobiol. Aging* 29, 848–855.
- Langers, D.R., Jansen, J.F., Backes, W.H., 2007. Enhanced signal detection in neuro-imaging by means of regional control of the global false discovery rate. *Neuroimage* 38, 43–56.
- Langsted, A., Freiberg, J.J., Nordestgaard, B.G., 2008. Fasting and nonfasting lipid levels: influence of normal food intake on lipids, lipoproteins, apolipoproteins, and cardiovascular risk prediction. *Circulation* 118, 2047–2056.
- Le Bihan, D., Mangin, J.F., Poupon, C., Clark, C.A., Pappata, S., Molko, N., Chabriat, H., 2001. Diffusion tensor imaging: concepts and applications. *J. Magn. Reson. Imaging* 13, 534–546.
- Lebel, C., Walker, L., Leemans, A., Phillips, L., Beaulieu, C., 2008. Microstructural maturation of the human brain from childhood to adulthood. *Neuroimage* 40, 1044–1055.
- Lee, J.E., Chung, M.K., Lazar, M., DuBray, M.B., Kim, J., Bigler, E.D., Alexander, A.L., 2009. A study of diffusion tensor imaging by tissue-specific, smoothing-compensated voxel-based analysis. *Neuroimage* 44, 870–883.
- Manolio, T.A., Ettinger, W.H., Tracy, R.P., Kuller, L.H., Borhani, N.O., Lynch, J.C., Fried, L.P., 1993. Epidemiology of low cholesterol levels in older adults. The Cardiovascular Health Study. *Circulation* 87, 728–737.
- Mauch, D.H., Nägler, K., Schumacher, S., Göritz, C., Müller, E.C., Otto, A., Pfrieger, F.W., 2001. CNS synaptogenesis promoted by glia-derived cholesterol. *Science* 294, 1354–1357.
- Mora, S., Rifai, N., Buring, J.E., Ridker, P.M., 2008. Fasting compared with nonfasting lipids and apolipoproteins for predicting incident cardiovascular events. *Circulation* 118, 993–1001.
- Morell, P., Jurevics, H., 1996. Origin of cholesterol in myelin. *Neurochem. Res.* 21, 463–470.
- Moseley, M., 2002. Diffusion tensor imaging and aging—a review. *NMR Biomed.* 15, 553–560.
- Mulder, S.D., Veerhuis, R., Blankenstein, M.A., Nielsen, H.M., 2012. The effect of amyloid associated proteins on the expression of genes involved in amyloid-beta clearance by adult human astrocytes. *Exp. Neurol.* 233, 373–379.
- Muldoon, M.F., Ryan, C.M., Matthews, K.A., Manuck, S.B., 1997. Serum cholesterol and intellectual performance. *Psychosom. Med.* 59, 382–387.
- Murphy, E.A., Roddey, J.C., McEvoy, L.K., Holland, D., Hagler Jr., D.J., Dale, A.M., Brewer, J.B., 2012. The Alzheimer's Disease Neuroimaging Initiative. CETP polymorphisms associate with brain structure, atrophy rate, and Alzheimer's disease risk in an APOE-dependent manner. *Brain Imaging Behav.* 6, 16–26.
- Natunen, T., Helisalmi, S., Vepsäläinen, S., Sarajarvi, T., Antikainen, L., Makinen, P., et al., 2012. Genetic analysis of genes involved in amyloid-beta degradation and clearance in Alzheimer's disease. *J. Alzheimers Dis.* 28, 553–559.
- Nir, T.M., Jahanshad, N., Villalon-Reina, J.E., Toga, A.W., Jack, C.R., Weiner, M.W., Thompson, P.M., 2013. Effectiveness of regional DTI measures in distinguishing Alzheimer's disease, MCI, and normal aging. *NeuroImage: Clin.* 3, 180–195.
- Page, R.M., Munch, A., Horn, T., Kuhn, P.H., Colombo, A., Reiner, O., Boutros, M., Steiner, H., Lichtenthaler, S.F., Haass, C., 2012. Loss of PAFAH1B2 reduces amyloid-beta generation by promoting the degradation of amyloid precursor protein C-terminal fragments. *J. Neurosci.* 32, 18204–18214.
- Parente, D.B., Gasparetto, E.L., da Cruz, L.C.H., Domingues, R.C., Baptista, A.C., Carvalho, A.C.P., Domingues, R.C., 2008. Potential role of diffusion tensor MRI in the differential diagnosis of mild cognitive impairment and Alzheimer's disease. *Am. J. Roentgenol.* 190, 1369–1374.
- Refolio, L.M., Menter, B., LaFrancois, J., Bryant-Thomas, T., Wang, R., Tint, G.S., Sambamurti, K., Duff, K., 2000. Hypercholesterolemia accelerates the Alzheimer's amyloid pathology in a transgenic mouse model. *Neurobiol. Dis.* 7, 321–331.
- Reid, P.C., Urano, Y., Kodama, T., Hamakubo, T., 2007. Alzheimer's disease: cholesterol, membrane rafts, isoprenoids and statins. *J. Cell Mol. Med.* 11, 383–392.
- Rodríguez-Rodríguez, E., Mateo, I., Infante, J., Llorca, J., García-Gorostiaga, I., Vazquez-Higuera, J.L., Sánchez-Juan, P., Berciano, J., Combarros, O., 2009. Interaction between HMGCR and ABCA1 cholesterol-related genes modulates Alzheimer's disease risk. *Brain Res.* 1280, 166–171.
- Rose, S.E., Chen, F., Chalk, J.B., Zelaya, F.O., Strugnell, W.E., Benson, M., Semple, J., Doddrell, D.M., 2000. Loss of connectivity in Alzheimer's disease: an evaluation of white matter tract integrity with colour coded MR diffusion tensor imaging. *J. Neurol. Neurosurg. Psychiatry* 69, 528–530.
- Rose, S.E., Andrew, L., Chalk, J.B., 2008. Gray and white matter changes in Alzheimer's disease: a diffusion tensor imaging study. *J. Magn. Reson. Spectrosc.* 27, 20–26.
- Roses, A.D., Lutz, M.W., Amrine-Madsen, H., Saunders, A.M., Crenshaw, D.G., Sundseth, S.S., Huettelman, M.J., Welsh-Bohmer, K.A., Reiman, E.M., 2010. A TOMM40 variable-length polymorphism predicts the age of late-onset Alzheimer's disease. *Pharmacogenomics J.* 10, 375–384.
- Ruggeri, R.B., 2005. Pharmacological inhibition for the modulation of plasma cholesterol levels and promising target for the prevention of atherosclerosis. *Curr. Top. Med. Chem.* 5, 257–264.
- Saher, G., Brugge, B., Lappe-Siefke, C., Mobius, W., Tozawa, R., Wehr, M.C., Wieland, F., Ishibashi, S., Klaus-Armin, N., 2005. High cholesterol level is essential for myelin membrane growth. *Nat. Neurosci.* 8, 468–475.
- Saher, G., Simons, M., 2010. Cholesterol and myelin biogenesis. *Subcell Biochem.* 51, 489–508.
- Schaefer, E.J., Audelin, M.C., McNamara, J.R., Shah, P.K., Tayler, T., Daly, J.A., Augustin, J.L., Seman, L.J., Rubenstein, J.J., 2001. Comparison of fasting and postprandial plasma lipoproteins in subjects with and without coronary heart disease. *Am. J. Cardiol.* 88, 1129–1133.
- Shobab, L.A., Hsiung, G.Y., Feldman, H.H., 2005. Cholesterol in Alzheimer's disease. *Lancet Neurol.* 4, 841–852.
- Solfrizzi, V., Panza, F., D'Introno, A., Colacicco, A.M., Capurso, C., Basile, A.M., Capurso, A., 2002. Lipoprotein(a), apolipoprotein E genotype, and risk of Alzheimer's disease. *J. Neurol. Neurosurg. Psychiatry* 72, 732–736.
- Solomon, A., Kareholt, I., Ngandu, T., Wolozin, B., Macdonald, S.W., Winblad, B., Nissinen, A., TuomiLehto, J., Soininen, H., Kivipelto, M., 2009. Serum total cholesterol, statins and cognition in non-demented elderly. *Neurobiol. Aging* 30, 1006–1009.
- Song, S.K., Sun, S.W., Ramsbottom, M.J., Chang, C., Russell, J., Cross, A.H., 2002. Dysmyelination revealed through MRI as increased radial (but unchanged axial) diffusion of water. *Neuroimage* 17, 1429–1436.
- Song, S.K., Yoshino, J., Le, T.Q., Lin, S.J., Sun, S.W., Cross, A.H., Armstrong, R.C., 2005. Demyelination increases radial diffusivity in corpus callosum of mouse brain. *Neuroimage* 26, 132–140.
- Sparks, D.L., 1997. Coronary artery disease, hypertension, ApoE, and cholesterol: a link to Alzheimer's disease? *Ann. N.Y. Acad. Sci.* 826, 128–146.
- Takahashi, S., Yonezawa, H., Takahashi, J., Kudo, M., Inoue, T., Tohgi, H., 2002. Selective reduction of diffusion anisotropy in white matter of Alzheimer disease brains measured by 3.0 Tesla magnetic resonance imaging. *Neurosci. Lett.* 332, 45–48.
- Tall, A.R., 1993. Plasma cholestryler ester transfer protein. *J. Lipid Res.* 34, 1255–1274.
- Tamnes, C.K., Ostby, Y., Fjell, A.M., Westlye, L.T., Due-Tonnessen, P., Walhovd, K.B., 2010. Brain maturation in adolescence and young adulthood: regional age-related changes in cortical thickness and white matter volume and microstructure. *Cereb. Cortex* 20, 534–548.
- Tatu, L., Moulin, T., Bogousslavsky, J., Duvernoy, H., 1996. Arterial territories of human brain: brainstem and cerebellum. *Neurology* 47, 1125–1135.
- Thomason, M.E., Thompson, P.M., 2011. Diffusion imaging, white matter, and psychopathology. *Annu. Rev. Clin. Psychol.* 7, 63–85.
- Turley, S.D., Burns, D.K., Rosenfeld, C.R., Dietschy, J.M., 1996. Brain does not utilize low density lipoprotein-cholesterol during fetal and neonatal development in the sheep. *J. Lipid Res.* 37 (9), 1953–1961.
- Ukmar, M., Makuc, E., Onor, M.L., Garbin, G., Trevisiol, M., Cova, M.A., 2008. Evaluation of white matter damage in patients with Alzheimer's disease and in patients with mild cognitive impairment by using diffusion tensor imaging. *Radiol. Med.* 113, 915–922.
- Vuletic, S., Jin, L.W., Marcovina, S.M., Peskind, E.R., Moller, T., Albers, J.J., 2003. Widespread distribution of PLTP in human CNS: evidence for PLTP synthesis by glia and neurons, and increased levels in Alzheimer's disease. *J. Lipid Res.* 44, 1113–1123.
- Waldstein, S., Elias, M., 2001. *Neuropsychology of Cardiovascular Disease*. Lawrence Erlbaum Associates, Mahwah, NJ.
- Warnick, G.R., Knopp, R.H., Fitzpatrick, V., Branson, L., 1990. Estimating low-density lipoprotein cholesterol by the Friedewald equation is adequate for classifying patients on the basis of nationally recommended cutpoints. *Clin. Chem.* 36, 15–19.
- Williams, V.J., Leritz, E.C., Shepel, J., McGlinchey, R.E., Milberg, W.P., Rudolph, J.L., Lipsitz, L.A., Salat, D.H., 2013. Interindividual variation in serum cholesterol is associated with regional white matter tissue integrity in older adults. *Hum. Brain Mapp.* 34, 1826–1841.
- Wollmer, M.A., Streffer, J.R., Lutjohann, D., Tsolaki, M., Iakovidou, V., Hegi, T., Pasch, T., Jung, H.H., von Bergmann, K., Nitsch, R.M., Hock, C., Papassotiropoulos, A., 2003. ABCA1 modulates CSF cholesterol levels and influences the age at onset of Alzheimer's disease. *Neurobiol. Aging* 24, 421–426.
- Xiao, Z., Wang, J., Chen, W., Wang, P., Zeng, H., Chen, W., 2012. Association studies of several cholesterol-related genes (ABCA1, CETP and LIPC) with serum lipids and risk of Alzheimer's disease. *Lipids Health Dis.* 11, 163.